

Size-tunable synthesis of gold nanorods using pyrogallol as a reducing agent

Yuanfu Huang^{1†}, Kai Xia^{1†}, Nongyue He^{1,2*}, Zhuoxuan Lu^{1*}, Liming Zhang¹, Yan Deng¹ & Libo Nie¹

¹Economical Forest Cultivation and Utilization of 2011 Collaborative Innovation Center in Hunan Province; Hunan Key Laboratory of Green Packaging and Application of Biological Nanotechnology; Hunan University of Technology, Zhuzhou 412007, China

²State Key Laboratory of Bioelectronics; School of Biological Science and Medical Engineering, Southeast University, Nanjing 210096, China

Received February 7, 2015; accepted March 10, 2015; published online June 25, 2015

A novel and facile seed-mediated method for the preparation of monodispersed gold nanorods (GNRs) is presented by introducing pyrogallol as a reductant. Fast Fourier transformation of high-resolution transmission electron microscopy reveals that the synthesized GNRs are single crystalline. The longitudinal surface plasmon resonance of GNRs can be finely tuned by varying silver ion concentrations or seed amounts. Also, both thick (diameter >30 nm) and thin (diameter <10 nm) GNRs with exceptional monodispersity can be well prepared by this method. These findings indicate that this method has a greater performance in controlling the morphology of GNRs than that of traditional approach with ascorbic acid as a reductant.

gold nanorods, seed-mediated, pyrogallol, size tunability

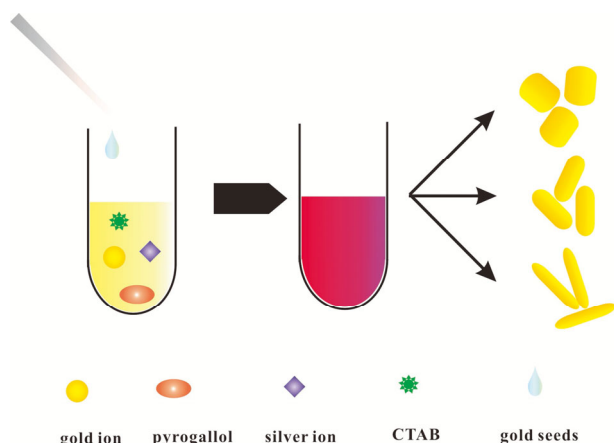
1 Introduction

Gold nanorods (GNRs) have received considerable attention, owing to their unique optical properties and potential applications in various fields such as plasmon-enhanced spectroscopies [1], sensing [2], biological imaging [3], photothermal therapy [3–7], drug delivery [8–10] and optical data storage [11]. To date, various approaches have been widely studied and improved for fabricating GNRs, such as templated method [12], electrochemical method [13], photochemical method [14], and seed-mediated growth method [15–18]. Among these, seed-mediated growth method, developed by Murphy *et al.* [15] and El-Sayed *et al.* [16], is the most common approach for the synthesis of GNRs. In a typical procedure, sodium borohydride is used to produce seed solution in Au(III)-cetyltrimethylammonium bromide

(CTAB) solution, and then an amount of seed solution is added to a group solution which contains Au³⁺, Ag⁺, CTAB and ascorbic acid (AA). Various factors, including pH value [19], temperature [20], bromide ions concentration [21], impurity in the CTAB [22], and additives [23–26], have been carefully evaluated by several research groups. However, one significant factor in nanorod synthesis, the type of reducing agent, has been rarely reported. In this paper, we firstly used pyrogallol instead of ascorbic acid as a reducing agent to prepare the GNRs (Scheme 1). The visible-near infrared (Vis-NIR) absorbance spectra of the as-prepared GNRs show that the longitudinal surface plasmon resonance (LSPR) of GNRs can be tuned from 630 to 880 nm. Transmission electron microscopy (TEM) results show the as-prepared GNRs with exceptional monodispersity can be well prepared by this method. Our approach offers a convenient and cost-effective way to prepare high monodispersed and uniform GNRs with tunable aspect ratio, which have a great potential for a range of applications, that is,

†Contributed equally to this work

*Corresponding authors (email: nyhe1958@163.com; luzhuoxuan1981@163.com)



Scheme 1 Schematic of seed-mediated synthesis of GNRs produced by pyrogallol as a reductant.

catalyst, optical polarizer, and ultrasensitive medical imaging technique.

2 Materials and experimental

Chloroauric acid, silver nitrate, pyrogallol, and sodium borohydride were purchased from Sinopharm Chemical Reagent Co. Ltd. (Shanghai, China), and CTAB was purchased from Sigma-Aldrich (USA). All chemicals were used without further purification and all solutions were prepared fresh daily. Furthermore, deionized water was used throughout all the work.

First, gold seeds were synthesized according to the previous literature [16]. HAuCl_4 solution (125 μL , 0.01 mol/L) was mixed with CTAB solution (5 mL, 0.1 mol/L), and a

fresh NaBH_4 solution (0.3 mL, 0.01 mol/L) was then injected into the Au(III)-CTAB solution under vigorous stirring. The solution developed a pale brown-yellow color, and the gold seeds were generated and kept for further use. Subsequently, to prepare the growth solution, certain volumes of silver nitrate (0.1 mol/L) solution were added to an HAuCl_4 solution (0.3 mL, 0.01 mol/L) in CTAB solution (7.125 mL, 0.1 mol/L), followed by adding certain volumes of pyrogallol aqueous solution, and the resulting mixture was hand-stirred until the solution color changed from yellow to pale rose red and then to pale brown-yellow. Finally, certain volumes of seed solution were injected into the growth solution under gentle stirring and left undisturbed at 30 °C for 12 h for nanorods growth. The Vis-NIR spectral measurement of GNRs was taken on a Shimadzu UV-3600 Spectrophotometer. TEM images were obtained on a JEM-2100 TEM. X-ray diffraction (XRD) patterns were measured on a Bruker D8-Advance diffractometer (Karlsruhe, Germany) using $\text{Cu K}\alpha$ irradiation. The high-resolution transmission electron microscopy (HR-TEM) image were taken in the Titan 80-300 transmission electron microscope (FEI, USA).

3 Results and discussion

In this study, gold seeds were synthesized with little modification according to the previous literature [16], and GNRs were prepared using both AA and pyrogallol as reductants under the same conditions (Figure 1). It should be mentioned that this novel preparation method shows greater advantages in controlling morphology of GNRs compared with traditional GNR preparation. Pyrogallol-reduced GNRs

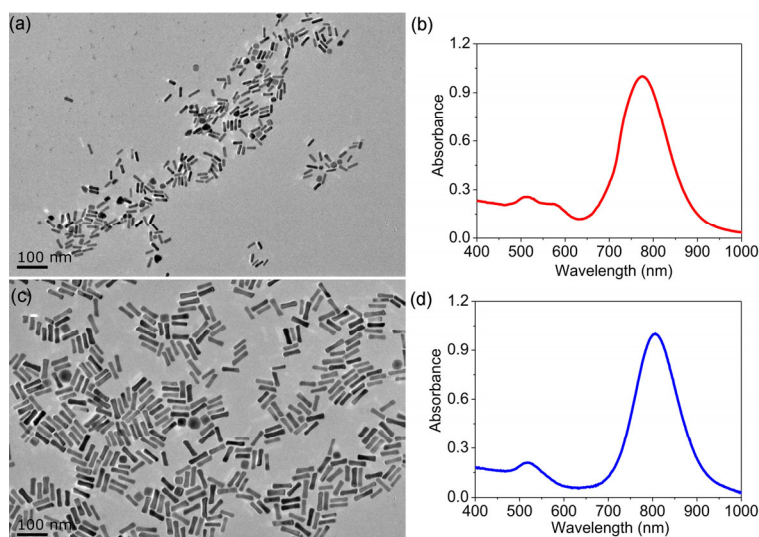


Figure 1 TEM images of GNRs prepared by AA (a) and pyrogallol (c) as reducing agents. The Vis-NIR spectra of the corresponding GNRs are shown in (b) and (d). GNR preparation conditions: (a) CTAB (0.1 mol/L, 7.125 mL), HAuCl_4 (0.01 mol/L, 0.3 mL), AA (0.1 mol/L, 48 μL), AgNO_3 (0.02 mol/L, 40 μL), and Seeds (40 μL); (c) CTAB (0.1 mol/L, 7.125 mL), HAuCl_4 (0.01 mol/L, 0.3 mL), pyrogallol (0.1 mol/L, 48 μL), AgNO_3 (0.02 mol/L, 40 μL), and Seeds (40 μL).

possess more monodispersed morphology compared with AA-reduced GNRs (Figure 1(a, c)). Accordingly, the corresponding LSPR peak of pyrogallol-reduced GNRs is sharper than that of AA-reduced GNRs (Figure 1(b, d)).

Considering that the unique optical characteristics of GNRs are governed by their aspect ratios, which are in turn affected by the silver ion concentration [16], we further investigated the effect of silver ions concentration via adding a serial concentration of silver nitrate solutions (from 0.027 to 0.105 mmol/L). The results indicated the aspect ratio of GNRs increased from 2.2 to 4.3 with increasing silver ion concentration. GNRs have a nearly identical rod-like shape with few spherical impurities (Figure 2(a–d)). Figure 2(e) shows the Vis-NIR absorption spectra of the GNRs with different amounts of silver nitrate using pyrogallol as a reducing agent. By increasing the volume of silver nitrate solution from 10 to 40 μL (0.02 mol/L), LSPR peak positions from 630 to 810 nm can be tuned. Because the LSPR peaks highly linearly depend on the aspect ratio, the controlled aspect ratio of the GNRs could finely tune LSPR

peak position.

The LSPR peaks can be fine-tuned across a broad spectral range not only by judiciously choosing the amount of silver ions, but also by varying seeds amount. As shown in Figure 3(e), the LSPR peak position of GNRs can be extended from 720 to 880 nm with increasing seed amount from 5 to 320 μL . TEM images in Figure 3(a–d) also demonstrated that the corresponding aspect ratios of the resultant GNRs augmented from 2.9 to 4.9, which are linearly related to LSPR (Figure 4). We found that GNRs with the dogbone morphology can be easily obtained with a small number of seeds (Figure 3(a)). The possible reason is that for a given gold ion concentration in the growth solution, the small number of seeds will lead to over-growth of GNRs [27]. With the overgrowth of GNRs, the {111} phase at the end of the rods breaks out of the CTAB shell and enlarges into the dogbone shape [28]. It should be mentioned that both length and width of GNRs were dramatically decreased when the seed amount was augmented. This is because that increasing seed amount leads to the increase in

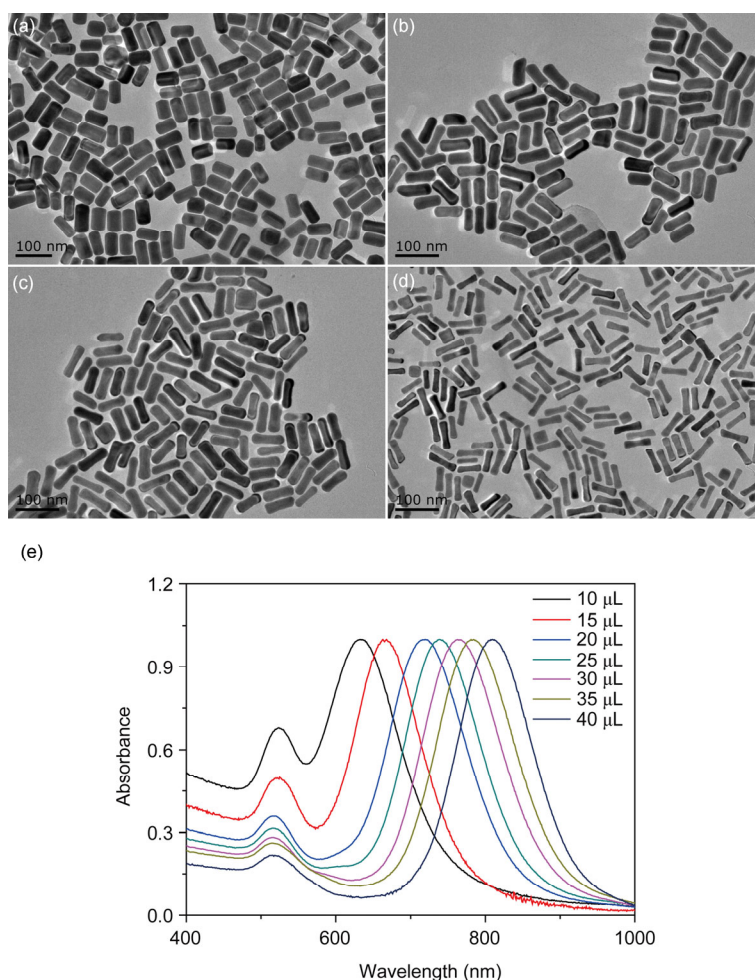


Figure 2 (a–d) TEM images of GNRs prepared by pyrogallol as a reducing agent with different amount of silver nitrate. GNRs preparation conditions: CTAB (0.1 mol/L, 7.125 mL), H₂AuCl₄ (0.01 mol/L, 0.3 mL), pyrogallol (0.1 mol/L, 45 μL), Seeds (40 μL), and different volumes of AgNO₃ (0.02 mol/L; (a) 10 μL , (b) 20 μL , (c) 30 μL , and (d) 40 μL). (e) Corresponding Vis-NIR spectra of GNRs prepared by pyrogallol as a reducing agent with different amounts of silver nitrate (color online).

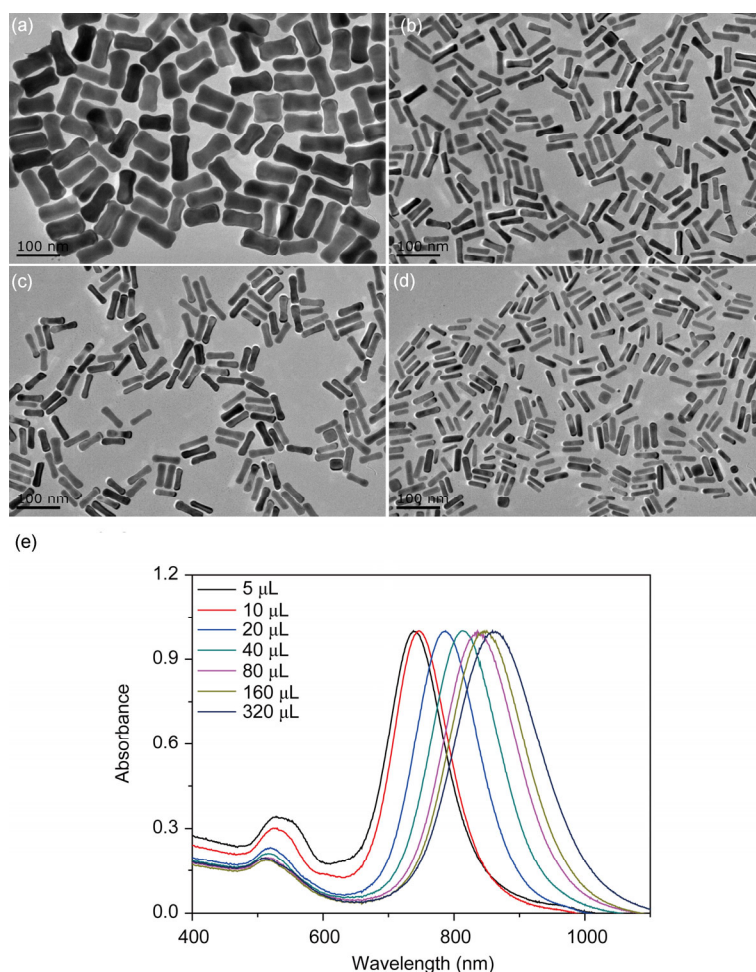


Figure 3 (a–d) TEM images of GNRs prepared by pyrogallol as a reducing agent with different amounts of seeds. GNR preparation conditions: CTAB (0.1 mol/L, 7.125 mL), H₂AuCl₄ (0.01 mol/L, 0.3 mL), pyrogallol (0.1 mol/L, 45 μL), AgNO₃ (0.02 mol/L, 40 μL), and different volumes of Seeds ((a) 5 μL, (b) 40 μL, (c) 80 μL, (d) 320 μL). (e) Corresponding Vis-NIR spectra of GNRs prepared by pyrogallol as a reducing agent with different amounts of seeds (color online).

the number of GNR particles. Therefore, for a given gold ions concentration, augmenting seed amount dictates the ultimate GNRs dimension. It is reported that larger GNRs have larger extinction coefficients, and might provide better performance in optical imaging applications, whereas smaller GNRs might provide improved coefficients in photothermal therapy applications that rely on turning incoming photons into outgoing heat, because of their improved absorption coefficients [29–31]. In our method, both thick (diameter >30 nm) and thin (diameter <10 nm) GNRs with exceptional monodispersity were well prepared by changing the seeds concentration (Table 1). Therefore, this new method has great potential for preparing high-quality GNRs for a wide range of applications.

It has been shown that the morphology of micellization formed by CTAB surfactant can be modulated through the addition of certain aromatic compounds such as sodium salicylate [31–33]. Ye *et al.* [24] reported that the addition of aromatic additives is favourable for the preparation of GNRs with tunable LSPR. Scarabelli *et al.* [34] studied the effect of salicylic acid on the synthesis of GNRs, both as a

Table 1 Sizes of GNRs in Figures 2 and 3

Silver ion (mmol/L)	Seeds (μL)	TEM figures	Length (nm)	Width (nm)
0.027	40	2(a)	59.2±5.5	26.5±2.3
0.054	40	2(b)	72.8±5.3	28.1±2.1
0.079	40	2(c)	73.3±4.9	21.5±2.4
0.105	40	2(d)	64.1±3.6	14.9±1.2
0.105	5	3(a)	99.2±6.1	33.7±2.8
0.105	40	3(b)	64.3±4.7	15.3±1.7
0.105	80	3(c)	62.4±4.7	14.4±1.6
0.105	320	3(d)	47.9±7.4	9.8±1.6

stabilizing cofactor and as a reductant. Therefore, in our system, pyrogallol not only can act as a reductant to reduce Au³⁺ to Au⁺ and help the growth of the gold seeds but also can penetrate into CTAB molecules and mediate the binding between CTAB and GNRs. We studied the effect of pyrogallol concentration on the growth of GNRs. Figure 5 shows the TEM images and the Vis-NIR absorption spectra of the GNRs with different amounts of pyrogallol, respectively. The results showed that the amount of pyrogallol does not

result in changing LSPR peak position but affects the intensity ratio of the LSPR to transverse surface plasmon resonance (TSPR) peak of GNRs. Using less pyrogallol volume (18 μL) led to a low-intensity ratio of LSPR to TSPR (Figure 5(e), black curve) indicating the presence of a lot of spherical or roughly spherical nanoparticles. The TEM images (Figure 5(a)) further confirmed it. GNRs with a higher ratio of LSPR to TSPR can be obtained when the concentration of pyrogallol increases from 0.2 to 0.6 mmol/L. However, excessively high concentration of pyrogallol instead leads to a lower ratio of LSPR to TSPR (more than 0.6 mmol/L, Figure 5(e), dark blue curve). The possible reason is that the high concentration of pyrogallol significantly increases the reducibility which leads to the very fast formation of growth units (Au⁰) and then results in the fast and uncontrolled growth of seed particles in all directions and forms more spherical particles.

To identify the structure of the synthesized GNRs, HR-TEM investigation (Figure 6) and XRD (Figure 7) analysis

were performed. Fast Fourier transformation of HR-TEM reveals that the synthesized GNRs are single crystalline (inset of Figure 6(a)). Lattice fringes parallel to the long axis of the nanorods can be discerned with d-spacings of

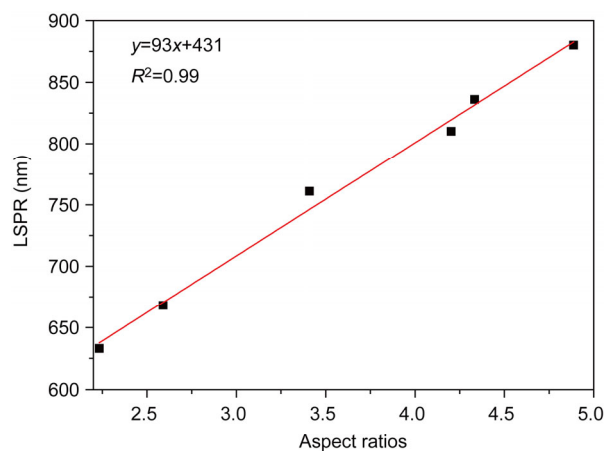


Figure 4 The linear relationship of LSPR and aspect ratios of GNRs.

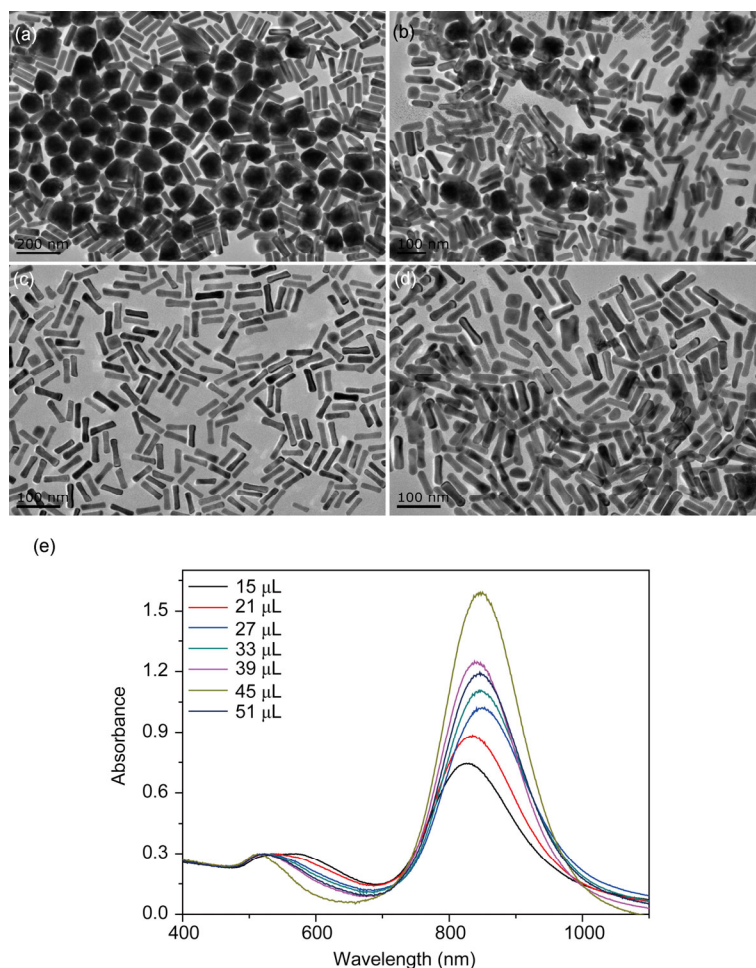


Figure 5 (a–d) TEM images of GNRs prepared by pyrogallol as a reducing agent with different amounts of pyrogallol. GNR preparation conditions: CTAB (0.1 mol/L, 7.125 mL), HAuCl₄ (0.01 mol/L, 0.3 mL), Seeds (40 μL), AgNO₃ (0.02 mol/L, 40 μL), and different volumes of pyrogallol (0.1 mol/L; (a) 15 μL , (b) 30 μL , (c) 45 μL , (d) 51 μL). (e) Corresponding Vis-NIR spectra of GNRs prepared by pyrogallol as a reducing agent with different amounts of pyrogallol. All scale bars represent 100 nm (color online).

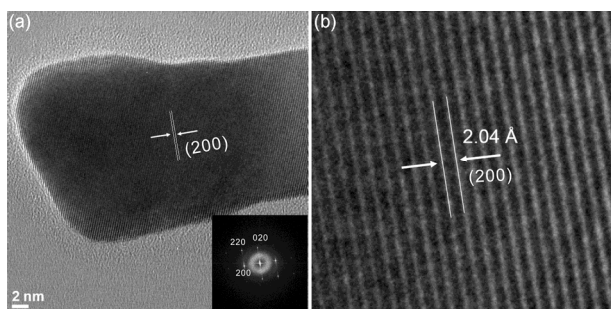


Figure 6 HR-TEM images of single GNRs. GNR preparation conditions: CTAB (0.1 mol/L, 7.125 mL), HAuCl₄ (0.01 mol/L, 0.3 mL), pyrogallol (0.1 mol/L, 45 μL), AgNO₃ (0.02 mol/L, 40 μL), and Seeds (40 μL).

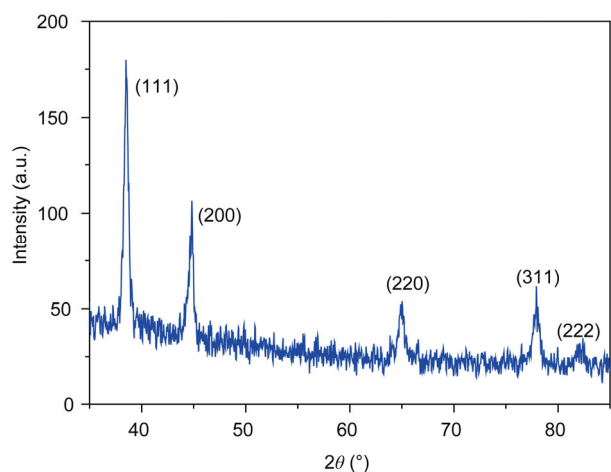


Figure 7 XRD pattern of the synthesized GNRs.

2.04 Å (Figure 6(b)) corresponding to the (200) lattice planes [35]. Five diffraction lines observed in the XRD pattern at $2\theta=38.5^\circ$, 44.8° , 64.9° , 77.9° , and 81.8° respectively correspond to (111), (200), (220), (311) and (222) reflections of the face-centered cubic structure of metallic gold (JCPDF No. 04-0784) [36].

4 Conclusions

In summary, we have demonstrated a highly versatile and efficient method for fabricating GNRs by introducing pyrogallol as substitute of AA into the well-established seed-mediated synthesis of GNRs. This new method produces high uniform and monodispersed GNRs with LSPR peak range from 630 to 880 nm. Also, both thick (diameter >30 nm) and thin (diameter <10 nm) GNRs with exceptional monodispersity can be fabricated. These findings indicate that pyrogallol has greater advantages in controlling the morphology of GNRs than AA as a reductant. Although gold and nanorod nanomaterials have been widely investigated recently [36–41], this new method has great potential for preparing high-quality GNRs for a range of applications including sensing applications, plasmon-enhanced spectroscopy, and photothermal cancer therapies.

This work was supported by the National Natural Science Foundation of China (61271056, 61301039, 61102031, 21205036), Hunan Provincial Natural Science Foundation of China (13JJ4091, 12JJ6060), China Post-doctoral Science Foundation funded projects (2014M550261, 2014T70459), the Scientific Research Fund of Hunan Provincial Education Department (13A003), and the Economical Forest Cultivation and Utilization of 2011 Collaborative Innovation Center in Hunan Province [(2013) 448].

- Lee A, Andrade GFS, Ahmed A, Souza ML, Coombs N, Tumarkin E, Liu K, Gordon R, Brolo AG, Kumacheva E. Probing dynamic generation of hot-spots in self-assembled chains of gold nanorods by surface-enhanced raman scattering. *J Am Chem Soc*, 2011, 133: 7563–7570
- Wang LB, Zhu YY, Xu LG, Chen W, Kuang H, Liu LQ, Agarwal A, Xu CL, Kotov NA. Side-by-side and end-to-end gold nanorod assemblies for environmental toxin sensing. *Angew Chem Int Ed*, 2010, 49: 5472–5475
- Huang XH, El-Sayed IH, Qian W, El-Sayed MA. Cancer cell imaging and photothermal therapy in the near-infrared region by using gold nanorods. *J Am Chem Soc*, 2006, 128: 2115–2120
- Huang YF, Sefah K, Bamrungsap S, Chang HT, Tan W. Selective photothermal therapy for mixed cancer cells using aptamer-conjugated nanorods. *Langmuir*, 2008, 24: 11860–11865
- Zhou WB, Shao JY, Qiao J, Wei QS, Tang JG, Jian J. Zwitterionic phosphorylcholine as a better ligand for gold nanorods cell uptake and selective photothermal ablation of cancer cells. *Chem Commun*, 2010, 46: 1479–1481
- Choi WI, Kim JY, Kang C, Byeon CC, Kim YH, Tee G. Tumor regression *in vivo* by photothermal therapy based on gold-nanorod-loaded, functional nanocarriers. *ACS Nano*, 2011, 5: 1995–2003
- Pandey S, Thakur M, Mewada A, Anjarlekar D, Mishra N, Sharon M. Carbon dots functionalized gold nanorod mediated delivery of doxorubicin: tri-functional nano-worms for drug delivery, photothermal therapy and bioimaging. *J Mater Chem B*, 2013, 1: 4972–4982
- Takahashi H, Niidome Y, Yamada S. Controlled release of plasmid DNA from gold nanorods induced by pulsed near-infrared light. *Chem Commun*, 2005, 17: 2247–2449
- Guo R, Zhang LY, Qian HQ, Li RT, Jiang XQ, Liu BR. Multifunctional nanocarriers for cell imaging, drug delivery, and near-IR photothermal therapy. *Langmuir*, 2010, 26: 5428–5434
- Kang HZ, Trondoli AC, Zhu GZ, Chen Y, Chang YJ, Liu HP, Huang YF, Zhang XL, Tan WH. Near-infrared light-responsive core-shell nanogels for targeted drug delivery. *ACS Nano*, 2011, 5: 5094–5099
- Zijlstra P, Chon JWM, Gu M. Five-dimensional optical recording mediated by surface plasmons in gold nanorods. *Nature*, 2009, 459: 410–413
- Martin CR. Membrane-based synthesis of nanomaterials. *Chem Mater*, 1996, 8: 1739–1746
- Yu YY, Chang SS, Lee CL, Wang CRC. Gold nanorods: electrochemical synthesis and optical properties. *J Phys Chem B*, 1997, 101: 6661–6664
- Kim F, Song JH, Yang PD. Photochemical synthesis of gold nanorods. *J Am Chem Soc*, 2002, 124: 14316–14317
- Jana NR, Gearheart L, Murphy CJ. Wet chemical synthesis of high aspect ratio cylindrical gold nanorods. *J Phys Chem B*, 2001, 105: 4065–4067
- Nikoobakht B, El-Sayed MA. Preparation and growth mechanism of gold nanorods (NRs) using seed-mediated growth method. *Chem Mater*, 2003, 15: 1957–1962
- Sau TK, Murphy CJ. Seeded high yield synthesis of short Au nanorods in aqueous solution. *Langmuir*, 2004, 20: 6414–6420
- Jana NR. Gram-scale synthesis of soluble, near-monodisperse gold nanorods and other anisotropic nanoparticles. *Small*, 2005, 1: 875–882
- Wang CG, Wang TT, Ma ZF, Su ZM. pH-tuned synthesis of gold nanostructures from gold nanorods with different aspect ratios.

- Nanotechnology*, 2005, 16: 2555–2560
- 20 Park HJ, Ah CS, Kim WJ, Choi IS, Lee KP, Yun WS. Temperature-induced control of aspect ratio of gold nanorods. *J Vac Sci Technol A*, 2006, 24: 1323–1326
 - 21 Garg N, Scholl C, Mohanty A, Jin RC. The role of bromide ions in seeding growth of Au nanorods. *Langmuir*, 2010, 26: 10271–10276
 - 22 Smith DK, Korgel BA. The importance of the CTAB surfactant on the colloidal seed-mediated synthesis of gold nanorods. *Langmuir*, 2008, 24: 644–649
 - 23 Ahmed W, Kooij ES, van Silfhout A, Poelsema B. Quantitative analysis of gold nanorod alignment after electric field-assisted deposition. *Nano Lett*, 2009, 9: 3786–3794
 - 24 Ye XC, Jin LH, Caglayan H, Chen J, Xing GZ, Zheng C, Doan-Nguyen V, Kang YJ, Engheta N, Kagan CR, Murray CB. Improved size-tunable synthesis of monodisperse gold nanorods through the use of aromatic additives. *ACS Nano*, 2012, 6: 2804–2817
 - 25 Ye XC, Gao YZ, Chen J, Reifsnnyder DC, Zheng C, Murray CB. Seeded growth of monodisperse gold nanorods using bromide-free surfactant mixtures. *Nano Lett*, 2013, 13: 2163–2171
 - 26 Ye XC, Zheng C, Chen J, Gao YZ, Murray CB. Using binary surfactant mixtures to simultaneously improve the dimensional tunability and monodispersity in the seeded growth of gold nanorods. *Nano Lett*, 2013, 13: 765–771
 - 27 Khlebtsov BN, Ithanadeev VA, Ye J, Sukhorukov GB, Khlebtsov NG. Overgrowth of gold nanorods by using a binary surfactant mixture. *Langmuir*, 2014, 30: 1696–1703
 - 28 Xu XD, Cortie MB. Shape change and color gamut in gold nanorods, dumbbells, and dog bones. *Adv Funct Mater*, 2006, 16: 2170–2176
 - 29 Lohse SE, Murphy CJ. The quest for shape control: a history of gold nanorod synthesis. *Chem Mater*, 2013, 25: 1250–1261
 - 30 Jain PK, Lee KS, El-Sayed IH, El-Sayed MA. Calculated absorption and scattering properties of gold nanoparticles of different size, shape, and composition: applications in biological imaging and biomedicine. *J Phys Chem B*, 2006, 110: 7238–7248
 - 31 Prescott SW, Mulvaney P. Gold nanorod extinction spectra. *J Appl Phys*, 2006, 99: 123504–123507
 - 32 Lin Z, Cai JJ, Scriven LE, Davis HT. Spherical-to-wormlike micelle transition in ctab solutions. *J Phys Chem*, 1994, 98: 5984–5993
 - 33 Hassan PA, Yakhmi JV. Growth of cationic micelles in the presence of organic additives. *Langmuir*, 2000, 16: 7187–7191
 - 34 Scarabelli L, Grzelczak M, Liz-Marzan LM. Tuning gold nanorod synthesis through pre-reduction with salicylic acid. *Chem Mater*, 2013, 25: 4232–4238
 - 35 Johnson CJ, Dujardin E, Davis SA, Murphy CJ, Mann S. Growth and form of gold nanorods prepared by seed-mediated, surfactant-directed synthesis. *J Mater Chem*, 2002, 12: 1765–1770
 - 36 Sun HM, Yuan QH, Zhang BH, Ai KL, Zhang PG, Lu LH. Gd-III functionalized gold nanorods for multimodal imaging applications. *Nanoscale*, 2011, 3: 1990–1996
 - 37 Wang SF, Zhang CF, Sun GA, Chen B, Xiang X, Ding QP, Zu XT. Chelating agents role on phase formation and surface morphology of single orthorhombic YMn_2O_5 nanorods via modified polyacrylamide gel route. *Sci China Chem*, 2014, 57: 402–408
 - 38 Wang C, Bao CC, Liang SJ, Fu HL, Wang K, Deng M, Liao QD, Cui DX. RGD-conjugated silica-coated gold nanorods on the surface of carbon nanotubes for targeted photoacoustic imaging of gastric cancer. *Nanoscale Res Lett*, 2014, 9: 264
 - 39 Zhen SJ, Guo FL, Li YF, Huang CZ. A facile one-pot method to fabricate gold nanoparticle chains with dextran. *Sci China Chem*, 2013, 56: 387–392
 - 40 Wang W, Liu C, Ling J, Huang CZ. Mercuric ions induced aggregation of gold nanoparticles as investigated by localized surface plasmon resonance light scattering and dynamic light scattering techniques. *Sci China Chem*, 2013, 56: 806–812
 - 41 Ye XS, Shi H, He XX, Wang KM, Li D, Qiu PC. Gold nanorod-seeded synthesis of Au@Ag/Au nanospheres with broad and intense near-infrared absorption for photothermal cancer therapy. *J Mater Chem B*, 2014, 2: 3667–3673